



**The Abdus Salam
International Centre for Theoretical Physics**



2060-48

**Advanced School on Non-linear Dynamics and Earthquake
Prediction**

28 September - 10 October, 2009

**Study of Seismic Regime in the Alps and Dinarides Junction Zone:
Block Structure Modeling and Historical observations**

I. Vorobieva

*International Institute of Earthquake Prediction Theory and Mathematical Geophysics
Moscow
Russia*

Study of strong seismicity in the Alps and Dinarides Junction zone: block structure modeling and historical observations

I. A. Vorobieva, A. Peresan, A. A. Soloviev and G. F. Panza.

Abstract

The block structure model is used to study long-term characteristics of strong seismicity at the junction zone of Alps and Dinarides. The fault-and-block geometry is outlined based on the morphostructural zoning map of the study area, as well as on the spatial pattern of the recorded seismicity. The model recovers the main features of observed seismicity and kinematics in the region that is checked against the available observations. A synthetic earthquake catalog with equivalent duration 75 thousand of years was generated,. The rate of extreme synthetic events with magnitude $M \geq 7$ is slightly lower than 2 events per 1000 years, and maximum magnitude is 7.4. Most of the extreme synthetic events is located along the southern boundary of Alps; another large group is located east of Istria peninsula. Several synthetic earthquakes with magnitude larger than 7 were generated along the Idrija line, and at the eastern and western boundaries of Northern Dinarides. Many of these locations already experienced significant historical earthquakes, with magnitudes greater than 6. The model evidences a number of possible locations for extreme events, where large earthquakes were not observed before; in particular several extreme events are generated at the western boundary of Dinarides nearby the city of Trieste. The obtained results do not contradict the available historical observations and are in good agreement with the earthquake prone areas, identified by morphostructural zonation and pattern recognition analysis, hence they can be useful for seismic hazard assessment.

1. Introduction

The study of the largest earthquakes is very important for estimation of the seismic hazard and seismic risk assessment, especially in the highly populated areas. In particular it includes identification of the potentially hazardous zones, estimation of the recurrence period, and of maximum possible magnitude of destructive earthquakes.

The junction zone of Southern Alps and Dinarides is one of the most seismically active territories in Europe. A number of destructive events occurred here. The largest instrumentally recorded earthquake occurred in Friuli, 1976, and had magnitude 6.5. Such earthquakes expose to seismic hazard the north-eastern part of Italy (Friuli-Venezia-Giulia), Slovenia and Croatia, and specifically, the cities of Trieste, Udine and Ljubljana.

The region has a long history of seismicity monitoring and has been intensively studied in the last decade. Several catalogs of significant historical earthquakes that cover zone of Alps-Dinarides junction are compiled: "Earthquake catalogue for Central and Southeastern Europe 342 BC - 1990 AD", (SHEBALIN et al., 1998); UCI (Peresan & Panza, 2002), "Catalogo Parametrico dei Terremoti Italiani (CPTI04)", (Gruppo di lavoro CPTI, 2004). A number of paleoseismic studies was carried out. Fitzko et al. (2005) found constraints that are consistent with the epicenter of the 1511 earthquake reported by Živčić et al. (2000). A first order identification of seismogenic nodes in Alps and Dinarides was carried out by Gorshkov et al., (2004); later on the geometry of nodes in the Alps-Dinarides hinge zone was delineated and the recognition of seismogenic nodes ($M \geq 6$) has been performed by Gorshkov et al., (2009)

In spite of intensive investigations, the reliable determination of possible localization of largest earthquakes, the estimation of the maximum magnitude and period of recurrence still remains an open problem. Available data cover more than one thousand of years, nevertheless, the duration of instrumentally recorded catalogs is several decades only. Historical catalogs based on the macroseismic observations and paleoseismic studies are less reliable, since they suffer from inhomogeneity and incompleteness. Accuracy of magnitudes and epicenters determination is poor. Fortunately, with progress of computer sciences and knowledge of earthquake generation a number of numerical models simulating seismicity have been developed.

In the present work we use the block structure model described in detail by Soloviev and Ismail-Zadeh (2003) to study strong seismicity in the zone of Alps-Dinarides junction. The block model provides a straightforward tool for a broad range of problems, like the study of the dependence of seismicity on the general properties of the fault networks and rheology, the formulation and testing of different hypothesis for seismic hazard assessment and earthquake

forecasting. The connection of geodynamics and seismicity is studied by Peresan et al. (2007), testing a number of hypotheses about tectonic processes that control the observed kinematics and seismicity in the Italian seismoactive region and its surroundings.

The method permits using a realistic geometry of the blocks, based on any relevant information. The tectonic motions can be prescribed using geodetic data (GPS, VLBI). The output of the modeling consists of kinematical data, i.e. the block movements that can be compared with observations (e.g. GPS), as well as of a synthetic earthquake catalog, where each event has origin time, coordinates of epicenter, magnitude and source mechanism. The synthetic earthquake catalog reproduces not only some of the basic global features of observed seismicity like (a) the Gutenberg-Richter law (e.g., Panza et al., 1997), (b) the space and time clustering of earthquakes (Maksimov and Soloviev, 1999) and (c) the dependence of the occurrence of large earthquakes on the fragmentation of the faults network, and on the rotation of blocks (Keilis-Borok et al., 1997), but also several regionally specific features of seismicity, like (1) the epicenter distribution, (2) the relative level of seismic activity in different areas of the region and (3) the type of fault plane solution.

The present work is devoted to study seismic regime at the junction zone of Southern Alps and Dinarides. The simultaneous analysis of the available observations and results of the numerical modeling allows get insights on the pattern of the large earthquakes occurrence, i.e. their possible locations, maximum magnitude and the period recurrence in the different parts of studied region.

2. The studied territory

Region is located in junction zone between eastern Alps and Dinarides. The region exhibits high seismicity, it is one of the most seismically active territories in Europe. The studied territory is shown in Figure 1. The region includes the Adria plate in the south, Southern Alps in the north and Dinarides in the east. The map of lineaments (Gorshkov et al., 2004) and seismicity with magnitude more than 4.0 (Peresan & Panza, 2002) is shown in the same Figure 1.

The major structural boundary between Alps and Dinarides is given by the first rank lineament (line I in Figure 1) traced along the latitude of the town of Tolmin; there, according to CAROBENE & CARULLI (1981) and CARULLI *et al.* (1990), the major tectonic orientation changes from Alpine to Dinaric. The location of this boundary is in agreement with other studies (PRELOGOVIĆ *et al.* 1998; POLJAK *et al.* 2001). This major discontinuity extends to the west by the overthrust boundary between Southern Alps and Friuli plain (lineament II in Figure 1). To the north the studied territory is bounded by the lineament of second rank that corresponds to the Periadriatic line (lineament III in Figure 1), which is a fault crosscutting a large part of the Alps

(D, 2000). The western boundary of the territory is the lineament IV that divides the Venetian Southern Alps into two megablocks, and corresponds to a sinistral strike-slip zone (MELETTI *et al.* 2000). The western and eastern limits of the Dinarides, the first rank lineaments V and VI in Figure 1, delimit the Dinarides from the Adriatic marine basin and Pannonian basin. Seismically active Idrija line that separates External and Internal Dinarides is represented by the third rank lineament VII (Figure 1). The transverse second rank E-W lineament VIII (Figure 1) intersects Dinarides and delimits more elevated areas to the south, from lower areas to the north. The lineament is traced along rectilinear segments of river valleys flowing in E-W direction. The second rank lineament IX (Figure 1) is traced along the Adriatic coast to the east of Istria peninsula. The territory is bounded to the south by the third rank lineament X that intersects Dinarides from west to east in the latitude 44.9°N

3. Observed seismicity: instrumental and historical data

Several earthquake catalogs are available for the studied territory. We use the catalog UCI (PERESAN & PANZA 2002) and its updates, referred in the following s UCI catalog, as a main data set. UCI catalog contains instrumentally recorded earthquakes as well as historical events, spanning a period of time from 1000 up to 2009, and covers completely the territory under study. UCI reports events with magnitudes more than 3.0 starting from 1870 for the most part the territory, excluding its southern part, south of latitude 45.5°, where earthquakes with magnitudes in range 3÷4.5 are systematically reported only after 1980. Before 1870, the catalog UCI reports historical data that are based essentially on the macroseismic observations.

The map of observed seismicity starting from magnitude 4 is given in Figure 1. The highest level of seismic activity in the study region is connected with the southern boundary of Alps, especially at the junction zone of Adria, Alps and Dinarides. High level of seismicity is observed also in the southern part of the region in the Adriatic coast to the east of the Istria peninsula.

The aim of the present work is to reproduce the main features of the largest earthquakes occurred in the past and, thus, to get some insights on the location and recurrence properties for earthquakes that may occur in the future. Therefore, additionally to the UCI catalog we analyze the historical large earthquakes reported in three other catalogs, namely: “Earthquake catalogue for Central and Southeastern Europe 342 BC - 1990 AD”, (SHEBALIN *et al.*, 1998) (we will refer it ECCSE); “Catalogo Parametrico dei Terremoti Italiani (CPTI04)”, (Gruppo di lavoro CPTI, 2004); and Global catalog NEIC, Significant Earthquakes World Wide Data file. The first catalog (SHEBALIN *et al.*, 1998) does not cover a small portion of the studied territory to the west of longitude 13°E. Other two catalogs cover completely region under study.

Each catalog mentioned above reports the number of significant earthquakes with magnitude 6.0 and more, and the sets of these events are different. All earthquakes that have magnitude more than 6.0 at least in one of the four catalogs are listed in Table 1. The coordinates of epicenters and magnitudes are given from all catalogs where the event is reported. Totally there are 21 large earthquakes.

Table 1. Significant earthquakes in Alps-Dinarides junction region.

<i>Date</i>	<i>UCI</i>		<i>ECCSE</i>		<i>CPTI</i>		<i>NEIC</i>					
<i>yyyy/mm/dd</i>	<i>epicenter</i>		<i>epicenter</i>		<i>epicenter</i>		<i>epicenter</i>					
		<i>M</i>		<i>M</i>		<i>M</i>			<i>M</i>			
567	-	-	45.60	15.30	6.2	-	-	45.6	15.3	-		
792 2 1	-	-	46.00	14.50	6.0	-	-	-	-	-		
1000 3 29	46.00	14.50	5.2	46.50	14.00	6.9	-	-	46.00	14.50	-	
1097	-	-	-	-	-	45.60	15.30	6.0	-	-		
1323	-	-	45.20	14.70	5.7	45.20	14.70	6.0	45.20	14.70	-	
1348 1 25	46.33	13.43	5.7	46.50	13.60	7.9	46.25	12.88	6.7	46.40	13.50	-
1511 3 26	46.13	13.70	5.7	46.20	13.80	7.4	46.20	13.43	6.5	46.10	14.00	6.9
1511 8 8	46.05	13.73	5.7	46.10	13.40	6.3	-	-	46.10	13.40	-	
1551 3 26	-	-	46.20	14.00	6.3	-	-	-	-	-		
1690 12 4	46.73	13.72	5.2	46.50	13.90	7.5	46.63	13.87	6.0	46.60	13.80	-
1721 1 12	-	-	45.30	14.40	6.1	45.30	14.40	6.00	45.30	14.40	-	
1870 3 1	-	-	45.50	14.50	6.4	45.40	14.40	5.6	-	-		
1873 6 29	46.15	12.38	6.3	-	-	46.15	12.38	6.3	46.10	12.30	-	
1895 4 14	46.13	14.53	5.6	46.05	14.50	6.1	46.13	14.53	6.3	46.10	14.50	6.1
1936 10 18	46.05	12.42	6.2	-	-	46.09	12.38	5.9	-	-		
1963 5 19	46.10	14.80	6.0	46.04	14.84	4.8	46.10	14.80	5.17	46.00	14.60	6.0
1976 5 6	46.23	13.13	6.5	46.3	13.2	6.5	46.24	13.12	6.43	46.35	13.27	6.5
1976 6 17	46.08	12.93	6.1	-	-	-	-	-	46.16	12.86	6.1	
1976 9 15	46.30	13.18	6.0	46.27	13.17	6.0	-	-	46.30	13.19	6.3	
1976 9 15	46.25	13.13	6.0	46.28	3.14	5.9	46.25	13.12	5.92	46.30	13.10	6.5
1998 4 12	46.24	13.65	6.0	-	-	46.07	13.35	5.70	46.25	13.65	6.0	

The maps of these earthquakes as they are reported in different catalogs are given in Figure 2. Earthquakes with magnitude 6.0 and more are marked by fill squares, events, which have magnitude less than 6.0 or undefined one, are marked by small crossed squares. Seismicity is shown in the scheme of morphostructural lineaments (Gorshkov et al., 2004). In spite of the

distribution of epicenters given by different sources appears quite different all of them correlate well with morphostructural lineaments.

The catalog UCI (Peresan & Panza 2002) (Figure 2a) does not report any significant earthquake in Dinaric part of the region; all events with magnitude 6.0 and above are located near the boundary between Alps and Dinarides and Alps and Friuli plain. Earthquake of 1690 that occurred in Periadriatic Line is reported with lesser magnitude $M=5.1$ (Table 1). Maximum magnitude reported in UCI is 6.5 for the 1976 Friuli earthquake.

The catalog ECCSE (Shebalin et al., 1998) (Figure 2b) reports large historical earthquakes over most of the study region, excluding most western part, which is not covered. In Dinaric part of territory large events sit in the Adriatic coast to the east of the Istria peninsula and in the boundary between Dinarides and Pannonian basin. Several events are reported in the boundary between Alps and Dinarides. The catalog presents information about a number of historical large events with magnitude more than 7.0, in particularly, the 1348 ($M=7.9$), and 1690 ($M=7.5$) earthquakes, that sit near the Fella-Salva line, but their location and magnitudes are disputable, as accuracy of the epicenter determination is poor for historical events. Shebalin et al. (1998) gives accuracy of epicenter determination $\pm 0.5^\circ$, and of magnitude determination ± 0.5 . Probably, these earthquakes had lower magnitudes and were connected with Periadriatic line (1690) or with boundary between Alps and Dinarides (1348), as they are reported in other three sources (see Table 1). Hammerl (1994) re-located the 1348 event from Carinthia to Friuli, and Postpischl (1985a) and Camassi & Strucchi (1996) placed it in Periadriatic line. Maximum magnitude reported in ECCSE is 7.9 and occurred in 1348.

The catalog CPTI (Figure 2c) reports number of significant earthquakes in the junction zone of Alps and Dinarides and Alps and Friuli plain, two large events in the Adriatic coast to the east of Istria (1323, 1721), and one at the boundary between Dinarides and Pannonian basin (1093) (Table 1). Maximum magnitude reported in CPTI is 6.7, 1348.

Global catalog NEIC (Figure 2d) reports all earthquakes with magnitude more than 6.0 at the boundary between Alps and Dinarides and Alps and Friuli plain. The number of significant events is reported in Dinaric part, but with undefined magnitudes (576; 1323; 1721) as well as earthquake of 1690 in Periadriatic line. Maximum magnitude reported in NEIC is 6.9, 1511.3.

In spite of significant earthquakes are reported in different way in the four sources it is possible conclude the following. Most seismically active area in the region is the boundary between Alps and Dinarides and Alps and Friuli plain, especially the junction of Alps, Dinarides and Adria. All the sources report a number of large events here. Instrumentally recorded large earthquakes Friuli 1976 and Bovec 1998 occurred here. The maximum level of recorded seismic activity is also observed in this zone. Another dangerous territory is Adriatic coast to the east of

Istria; three of four used sources report significant earthquakes here. The level of instrumentally recorded seismicity is also just high.

Information about significant earthquakes in Periadriatic line is less reliable, ECCSE gives magnitude $M=7.5$ and CPTI $M=6.0$ for the earthquake of 1690 that occurred here. Some investigators (Postpischl, 1985, Camassi & Strucchi, 1996) placed here the earthquakes 1348, but uncertainty of its epicenter is very large (see table 1). The level of instrumentally recorded seismicity is not high as well.

The estimation of the maximum possible magnitude and period of recurrence of largest events is still open problem. Maximum instrumentally recorded magnitude is 6.5 (Friuli 1976), and only one of four considered sources ECCSE reports historical events with magnitude more than 7 (Table 1). Maximum is $M=7.9$ in 1348, but it seems overestimated. At the same time the equivalent magnitude of the instrumentally recorded Friuli series (1976) is estimated more than 7. This fact suggests that the structure is able to generate earthquake with magnitude 7 or more, in spite of the absence of reliable recorded data. The period of the recurrence of the largest earthquakes in the region can be thousands of years; that is much larger than duration of observation, even including historical data. The realistic numerical modeling allows generating very long earthquake catalogs with duration tens thousands of years; this gives the possibility to estimate the long term features of seismicity in the studied region.

4. Basic elements of the numerical block structure model

The numerical model of the block structure dynamics and seismicity was introduced by Gabrielov et al. (1990) and described in details by Soloviev & Ismail-Zadeh (2003).

The main elements of modeling are the following.

1. The region is modeled as a system of perfectly rigid blocks that are separated by infinitely thin viscous-elastic fault planes that can have arbitrary dip angle. This assumption is justified by the fact that in the lithosphere the effective elastic moduli of the fault zones are significantly smaller than the ones within the blocks and it is rather realistic for short (as compared with the geological history) periods of simulation (thousands of years). The viscous-elastic features can be prescribed different for the different faults and block bottoms. As the blocks are perfectly rigid all deformation and stresses are concentrated in the fault planes and in the block bottoms.

2. The movement of the blocks is a consequence of the external motions, that are prescribed at the lateral boundaries and at the bottom of the structure. The directions of these movements are assumed to be horizontal. This assumption is supported by Cuffaro et al. (2006), who showed that the steady faster horizontal velocity of the lithosphere with respect to the upward or downward velocities at plate boundaries supports dominating tangential forces acting on plates.

The movement of the blocks obtained as the result of modeling also assumed to be horizontal. Nevertheless the model is not two-dimensional, because any direction of slippage is allowed in the fault planes, and it can have vertical component. This contradiction is resolved as following: all movements in the structure are assumed to be infinitely small comparing with the size of blocks, and it is very realistic, because the rate of tectonic motions is cm/yr or even mm/yr, and size of blocks is at least several tens of kilometers. As a result the geometry of the block structure does not change during the modeling. It means that model is intended for simulation of seismicity in the “short” non-geological period of time (tens thousands of years), when the geometry of the fault network in the region is not change. The movement rates and directions of the underlying medium can be different for each block bottom, as well as in the each segment of the lateral boundary of the block structure. The prescribed motions are assumed to be stationary and do not change in the process of modeling.

3. Earthquakes are allowed only in the fault planes. Each segment of the fault plane is divided into small cells. Earthquakes in the model occur in accordance with the dry friction law: when the ratio of shear to normal stress exceeds certain level in the cell of the fault plane an abrupt inelastic slippage occur in this cell. This abrupt inelastic displacement is interpreted as an earthquake. If many cells in the same fault simultaneously reach this critical level they join to the single event. For each synthetic earthquake the model provides: coordinates of hypocenter, magnitude and fault plane solution. The coordinates of the hypocenter are determined as the weighted sum, with weights proportional to the areas of the failed cells, of the coordinates of the cells forming the earthquake. The coordinates of hypocenter determined in this way are closer to the coordinates of centroid than epicenter under its classical definition, where it is the starting point of the rupture. This method of epicenter determination is used in the model, as synthetic earthquake occurs instantly: the all cells that reach critical state rapture simultaneously and impossible to determine which is the first one. The consequence of this determination of hypocenter is that large synthetic earthquakes are always in the middle of segment, as they are formed by large part of the segments’ cells.

The magnitude of the earthquake is calculated from Utsu and Seki, (1954):

$$M = 0.98 \log_{10} S + 3.93 \quad (6)$$

where S is the total area of the cells forming the earthquake, measured in km^2 .

The source mechanism is described by three angles: strike, dip, and slip. Two first ones are determined by the block structure geometry as azimuth and dip angle of the fault, where earthquake occurs. The slip angle can be determined considering the average vector of slippage in the failed cells.

4. Dimensionless time is used in the model. All variables containing time are referred to one unit of the dimensionless time, and the real time corresponding to the unit of the dimensionless time can be estimated at the interpretation stage of the results, comparing the velocities of block movements and intensity of the synthetic earthquake flow with available observations.

5. The input data for modeling are:

- Geometry of the block structure that includes fault network, dip angles of faults and depth (thickness) of the structure;
- Rates and direction of tectonic motions at the lateral boundaries and at the bottom of the structure;
- Rheological parameters that describe viscous-elastic features of the fault planes and block bottoms and conditions of earthquake occurrence.

The output of the modeling is synthetic earthquake catalog and movements of the blocks.

As any sort of numerical modeling the block structure model does not pretend to recover the observation in all the details. It assumes very simplified description of the studied region. The region is represented as a system of perfectly rigid blocks. Fault zone that has complex fractural structure and includes many small faults is presented as single infinitely thin plane with homogeneous features. Tectonic motions prescribed in the lateral boundaries and bottom of the block structure supposed to be horizontal and stationary. The model does not take into account inhomogeneous deep structure of the studied region. The simplified description of the region imposes a restriction to ability of the model in the detailed reproducing of the observation. Block structure model is able to reproduce long-term integral characteristics of seismicity and tectonic motions in the region They are directions and rates of block motions, correspondence between the rate of movements and intensity of earthquake flow, frequency-of occurrence relation, distribution of epicenters in the scale of the fault zones, relative level of seismic activity in the different parts of region, type of the source mechanism. Model does not pretend to reproducing subtle features of seismicity that are connected with regional system of the small fault that are not included in the block structure, as well as realistic depth distribution of the synthetic earthquakes, because rheological parameters of faults do not change with depth and movements of blocks are horizontal.

Based on the available observations (structural and tectonic schemes of the region, GPS measurements, recorded earthquake catalogs, etc.) the input parameters for modeling can not be determined by unique way, because observations have limited accuracy and allow different interpretations. The criterion of the modeling quality is reproducing of the main features of the observed seismicity and tectonic motions in the region under study. They are directions and rates of the block motions, correspondence between the rate of movements and intensity of earthquake

flow, distribution of epicenters, relative seismic activity in the different parts of region, type of the source mechanism. The recovering of the observations is obligatory condition while studying real region regardless of the sort of problem that is investigated by means of modeling.

5. Block model of the Alps and Dinarides junction region

To outline the fault-and-block geometry we use the morphostructural zoning map of the Alps and Dinarides (Gorshkov et al., 2004) as well as spatial pattern of the recorded seismicity. (Figure 1). The comparison of the morphostructural map with the recorded seismicity shows that large clusters of earthquakes and especially strong ones correlate with lineaments shown in Figure 1, therefore we can use morphostructural scheme as a base to model seismicity in the Alps and Dinarides junction region.

We trace the faults of the block structure along all lineaments of the first and second rank. We also include some lineaments of third rank; they are Idrija line, as it is significant seismogenic fault, and lineament X (Figure 1) intersecting Dinarides to bound the block structure in the south. The block structure consists of six blocks (Figure 3) that are outlined by 16 faults. The SW boundary of the structure corresponds to the first rank lineaments II and V, which separate the Alps and Dinarides from the Adria plate and second rank lineament IX that is traced along the Adriatic coast. Northern boundary of the structure is the Periadriatic line (second rank lineament III), while the western boundary is lineament IV in Venetian Southern Alps. Eastern boundary is traced along the lineament VI separating the Dinarides and Pannonian basin. Southern boundary is lineament X

Two blocks in the north (B1 and B2 in Figure 3) represent the Southern Alps. Four southern blocks (B3-B6 in Figure 3) represent the Dinarides. Transversal second rank lineament VIII intersects Dinarides in E-W direction and separates two northern blocks from two southern ones. The Idrija line (lineament of the third rank) divides the structure into western and eastern parts.

Ten boundary blocks are introduced to prescribe external forces acting in the region. Boundary blocks BB1 and BB2 bound structure from the west and north respectively. Boundary block BB3 is eastern limit of the structure crossing the Alps. BB4, BB5 represent eastern edge of Dinarides, BB6 is southern boundary of structure. BB7-BB10 represent the boundary of Adria plate.

To define depth of the block structure the information about distribution of seismicity in the depth (Figure 4) is used. Most part of events has depth within 20km, but seismicity extends till 40km. Another data are structural model of Italy (Chimera et al., 2003; Panza & Raikova, 2008). Two structural boundaries could be distinguished in the studied region: the first one is

Moho in the depth about 40 km that is in agreement with European Moho map (Cloetingh et al., 2006). Another structural boundary has depth about 20-25km. Thus the available information allows choose the thickness of layer 40km or 20km. The goal of the present work is study of strongest earthquakes in the region. We suppose that the whole volume till Moho is involved into generation of the strongest shocks, so preferable depth of the block structure corresponds to Moho, i.e. it is 40km.

The proper choice of the dip angles of the faults is essential for modeling. In correspondence with seismotectonic model of Garulli et al. (1990), the Idrija line and Periadriatic line are subvertical faults, while the line separating Southern Alps from Friuli plane and Dinarides is overthrust, and it is inclined fault. To define dip angles more precisely the information about fault plane solutions (FPS) is used. The Friuli earthquake of 1976 occurred in the overthrust line (fault 10 of the block structure), its FPS shows reverse faulting mechanism and dip angle about 30 degrees (Aoudia et al., 2000). Another large earthquake, Bovec, 1998, occurred to the east of Friuli 1976, where Idrija line (Fault 14 of the structure) intersects the boundary between Alps and Dinarides. It has right lateral strike-slip mechanism and subvertical dip angle (Bajc et al., 2001). To estimate dip angles for the whole structure the FPS from DST Data Base in the territory under study are associated with the faults of block structure. The FPSs are chosen by strike that corresponds to azimuth of the fault in the structure. The average dip angles are determined for each fault. The data are most reliable for Southern boundary of Alps (faults 10, 11, 16), Idrija line (fault 14) and western boundary of structure (fault 1). There are no FPS data for some faults. The following values of dip angles were chosen (Table 2)

Table 2. Dip angles of faults.

<i>Fault</i>	<i>Average dip angle from FPS</i>	<i>Dip angle in the model</i>	<i>Fault</i>	<i>Average dip angle from FPS</i>	<i>Dip angle in the model</i>
1	88.7	88	9	62.0	70
2	86.0	85	10	33.5	35
3	69.0	70	11	34.5	35
4	60	70	12	-	45
5	-	80	13	90.0	85
6	-	60	14	69.5	70
7	-	80	15	-	80
8	-	80	16	47.0	45

The viscous-elastic features are the same for all block bottoms: elastic coefficient $K=1.0$, coefficients controlling viscosity $W=0.07$. The viscous-elastic features of the faults' segments depend on the rank of the correspondent morphostructural lineament. We suppose that larger lineaments present more fractured zones, so rate of inelastic displacements should be higher. The

values are: $W=0.08$; $W_s = 80.00$ in the all segments of faults that correspond to the first rank lineaments; they are two times less in segments that correspond to the second rank lineaments, $W=0.04$, $W_s = 40.00$; and they are $W=0.02$, $W_s = 20.00$ in segments that correspond to the third rank lineaments. The special values are prescribed for two small segments, which are placed in the highly fractured zones of intersection of the large faults; they are junction zone of Adria, Alps and Dinarides, and intersection of Idrija line with the boundary between Alps and Dinarides. Here the values are two times more: $W=0.16$, $W_s = 160.00$. The ratio of shear to normal stress controlling earthquake occurrence in the model is: $B = 0.10$, $Hf = 0.085$, $Hs = 0.07$ and they are the same for all the segments. The list of values is given in Table 3; the numbers of segment are marked in the Figure 3.

Table 3 Viscous-elastic parameters of faults' segments.

<i>Segments</i>	<i>K</i>	<i>W</i>	<i>W_s</i>
8, 17, 18,23, 25	1.0	0.02	20
1-4, ,9, 19,21,22	1.0	0.04	40
5-7, 10-12, 14-16, 20, 26	1.0	0.08	80
13, 24	1.0	0.16	160

The size of the cell $\epsilon=2\text{km}$ that allows model seismicity from magnitude 4.

The movement of the Adria in the north direction with the velocity 3-4.5 mm/yr (Nocquet & Calais, 2003) is supposed to be the basic factor controlling geodynamics and seismicity in the studied region. To choose the direction and relative values of the velocities in the boundary of structure we used the GPS observations (D'Agostino et al., 2005; Nocquet & Calais, 2003). Accordingly to D'Agostino et al., (2005) the movement of Adria has some western component, authors estimate azimuth as -10° and rate about 3mm/yr in the vicinity of Trieste. The value of velocity decreases to the west of the region to 2mm/yr, and near Venice change direction to the north (D'Agostino et al., 2005; Nocquet & Calais, 2003). This allows prescribe the external velocities in boundary of Adria plate (Boundary blocks VII-X).

Dinarides are involved in NNW movement, with the lesser velocity (D'Agostino et al., 2005). We suppose, that velocity in Dinaric part of the region decreases from west to east, and small north directed movement is in the eastern boundary of Dinarides. Two knee-like bends break the boundary between Alps and Dinarides (see morphostructural scheme in Figure 1) strike and shift it in an en-echelon way to the south. According to Šušteršič (1996), the largest dextral offset inferred to the Idrija fault near Tolmin is about 12km. Another smaller bend is near Ljubljana. It is supposed, that the offset is due to the dextral cumulative displacement in the

Dinarides. Basing on this information we prescribe velocities in the southern and eastern boundary of the structure (boundary blocks IV-VI)

The observed velocities in the Alpine part of the region are much lesser than in Dinaric part. GPS observation (D'Agostino et al., 2005) show north directed velocity less than 1mm/yr inside of studied region. The Periadriatic line that delimits the block structure in the north is right lateral strike-slip zone. Nocquet & Calais (2003) give the NEE direction of velocity with the rate about 0.5mm/yr in the Central Alps, north from Periadriatic line, at HFLK site, situated to the NW from studied territory. D'Agostino et al. (2005) give a similar velocity at VKLM site situated near north-eastern corner of block structure.

On the base of information mentioned above we prescribe the following velocities for ten boundary blocks (Table 4). The dimensionless time is used while modeling, only directions and relative values are taken into account.

Table 4. Prescribed velocities of boundary blocks in *cm* per unit of dimensionless time

Boundary block	Description	V_x (East)	V_y (North)
1	Western boundary, Alps	0.0	0.0
2	Northern boundary, Periadriatic line	8.0	5.0
3	Eastern boundary, Alps	0.0	0.0
4	Eastern boundary, Dinarides, north	-1.0	9.0
5	Eastern boundary, Dinarides, south	-2.0	13.0
6	Sothern boundary, Dinarides	-5.0	25.0
7	Adriatic coast, east from Istria,	-7.0	50.0
8	Adria-Dinarides boundary	-8.0	50.0
9	Friuli plane – Dinarides boundary	-9.0	50.0
10	Friuli plane – Alps boundary	0.0	30.0

No velocities are prescribed for medium underlying all the blocks.

6. Results of modeling

The modeling was carried out for 600 units on of dimensionless time. All stresses and deformation are equal to zero at the initial moment of time, therefore we ignore the beginning part of catalog, first 100 units of time, and will consider the results obtained for 500 units of time, from 100 to 600, when movements in the structure and seismic regime become stabile.

6.1 The general features of synthetic seismicity

We obtained 113077 synthetic earthquakes in the magnitude range 4- 7.4. Experimental magnitudes are good to one digit, , therefore the synthetic magnitudes were also rounded off to one digit. The frequency of occurrence graph (Gutenberg-Richter plot) is given in the Figure 4, as well as observed relation that is constructed by UCI catalog for the period 1870-2006 when catalog is representative for magnitude 4.0. The plot for synthetic seismicity is pretty good linear in the range of magnitudes 4.2 – 7.0, and has almost the same slope as the plot of observed seismicity. The best fit linear relations for observed and synthetic seismicity are:

$$\lg(N) = -0.956 M + 6.426; \quad \sigma = 0.113 \quad \text{Observed}$$

$$\lg(N) = -0.965 M + 9.167; \quad \sigma = 0.055 \quad \text{Synthetic}$$

As *b*-values for observed and synthetic seismicity are the same, we can estimate the real-time duration of modeling.

$$T=10^{(9.168 - 6.424)} \cdot 136\text{yr} \approx 75\ 000\text{yr}; \text{ one unit of dimensionless time is } 150\text{yr}.$$

Below we describe and discuss the result of modeling rescaled to the real time.

6.2 Movement in the block structure.

The movements of the blocks of the structure are given in Table 5

Table 5 Velocities of blocks obtained from modeling.

<i>Blocks of structure</i>	<i>V_x, mm/yr (East)</i>	<i>V_y, mm/yr (North)</i>	<i>Boundary blocks</i>	<i>V_x, mm/yr (East)</i>	<i>V_y, mm/yr (North)</i>
B1	0.03	0.42	BB1	0.00	0.00
B2	0.01	0.39	BB2	0.60	0.33
B3	0.04	1.58	BB3	0.00	0.00
B4	-0.16	1.59	BB4	-0.07	0.60
B5	-0.17	1.91	BB5	-0.13	0.87
B6	0.01	1.95	BB6	-0.27	1.67
			BB7	-0.46	3.33
			BB8	-0.53	3.33
			BB9	-0.60	3.33
			BB10	0.00	2.00

Blocks 1 and 2 representing Alps move very slowly in north direction, with the velocity about 0.4mm/yr. Four blocks (B3-B6) representing Dinarides move much faster. The general direction of movement is north, the western blocks (B5, B6) move faster than eastern ones (B3, B4) and their velocities have small western component. The rate of velocity is 1.5 – 2mm/yr. Velocity of Adria is 3-3.5 mm/ per year at the eastern coast Adriatic Sea, and 2mm/yr near

Venice. The obtained values are in accordance with the observations (i.e. D'Agostiono et al., 2005, Jimenez-Munt et al., 2003, Nocquet et al., 2003.)

6.3 Regionally specific features of synthetic seismicity.

The spatial distribution of synthetic seismicity is presented in the Figure 5. The distribution of epicenters is similar to the observations (Figure 1). The most seismically active zone is boundary between Alps and Friuli plain an Alps and Dinarides.

The detailed information about number of events, maximum magnitude, and focal mechanisms of synthetic events that occur in the different faults of the structure is given in the Table 6. Events of maximum magnitude $M=7.4$ occurred in the boundary between Alps and Dinarides (fault 12, segment20) and in Idrija line (Fault 14, segment 23).

Table 6. Number of events, maximum magnitude and FPS of synthetic events

<i>Segment</i>	<i>Fault</i>	<i>Left block</i>	<i>Right block</i>	<i>Number of events</i>	<i>Maximum magnitude</i>	<i>Mechanism Slip angle</i>
1	1	bb1	b1	2627	5.9	-5
2	2	bb2	b1	0	-	-
3	2	bb2	b2	4241	6.6	170
4	3	bb3	b2	8152	6.4	115
5	3	bb4	b3	10963	7.0(1)*	115
6	4	bb4	b3	4720	7.2(5)	125
7	4	bb5	b4	0	-	-
8	5	b4	b6	0	-	-
9	7	b5	bb8	314	6.9	105
10	8	b5	bb8	608	6.8	140
11	8	b6	bb8	517	7.2(4)	140
12	9	b6	bb9	10408	7.1(1)	135
13	9	b1	bb10	9906	6.6	125
14	10	b1	bb10	10685	7.0(2)	105
15	11	b1	bb10	3047	7.1(16)	65
16	15	b4	bb6	6040	6.4	140
17	15	b4	b5	933	5.7	150
18	15	b3	b6	653	5.3	155
19	6	b5	Bb7	7537	7.0(17)	125
20	12	b2	b3	6327	7.4(49)	95
21	13	b3	b4	0	-	-
22	13	b6	b5	0	-	-
23	14	b3	b6	1809	7.4((15)	130
24	14	b2	b6	1414	6.6	125
25	14	b2	b1	0	-	-
26	16	b1	b6	22828	7.2(30)	100

*Number of events with magnitude 7.0 and more generated in the segment

The direct comparison of the relative seismic activity in the different territories is difficult, as it is impossible to assign an observed event to the certain segment of the block structure in unique way. To overcome this difficulty we divide the studied region into 10 sub-regions. The scheme is given in Figure 6, as well as observed seismicity from magnitude 3 (UCI, 1870-2006). In spite we model the seismicity from magnitude 4, we use observed seismicity from magnitude 3 to obtain more reliable estimation of relative activity, as number of recorded earthquakes with magnitude 4 is small – 330 events. Sub-region number 10 is aseismic, only 3 events are reported in UCI, and it is not a consequence of the catalog incompleteness, as global catalog NEIC also reports only two events here. The analysis of data shows that catalog UCI is quite complete for all the territories, excluding sub-region 9, it means that real level of activity (number of events) is higher, than reported in UCI. The result of comparison is presented in Table 7.

Table 7. Relative seismic activity in the different territories

<i>N</i>	<i>Sub-region</i>	<i>Number of observed EQ</i>	<i>% of observed EQ</i>	<i>Number of synthetic EQ</i>	<i>% of synthetic EQ</i>
1	Periadriatic line	67	2.8	4241	3.7
2	Alps western and southern boundary	333	13.8	5674	5.1
3	Junction zone Alps-Dinarides-Adria	1087	44.9	44833	39.7
4	Alps eastern boundary	124	5.2	8152	7.2
5	Alps-Dinarides boundary	328	13.6	17290	15.3
6	Dinarides, western boundary, north	159	6.6	11533	10.2
7	Idrija line	121	5.0	2740	2.4
8	Dinarides, eastern boundary, north	111	4.6	4720	4.2
9	Dinarides, western boundary, south	123	5.1	14824	13.1
10	Dinarides, eastern boundary, south	3	0.1	0	0.0

The most active is sub-region 3, the zone of Alps-Dinarides-Adria junction. 44.9% of observed and 39.7% and synthetic earthquakes respectively are located here. The level of observed seismicity is a bit higher, than synthetic one. It can be a consequence of 1976 Friuli earthquake with good reported huge aftershock sequence that occur here. The Friuli swarm occupies about 15% of the all recorded events in the region under study. Model generates the low number of events in two sub-regions in Idrija line (sub-region 7), and in western part of boundary between Alps and Friuli plain (sub-region 2). The relative number of synthetic

earthquakes, more than two time less than observed ones. But synthetic earthquakes are very strong in these zones, maximum magnitude excides 7, so the level of synthetic seismic activity is not low here; it is some lack of the small events. The relative number of synthetic earthquakes in Adriatic coast east to Istria (sub-region 9) is more then two times larger, than observed one, it can be a consequence of the UCI incompleteness in this zone. The estimation of the relative activity by observed magnitude 4.5 gives 10%, that is close to the obtained from modeling 13.1%. Taking into account that any large event with aftershock sequence can change considerably the relative level of seismic activity of the zone where it occur, we can consider the space distribution of synthetic seismicity as a good corresponding to the observations.

The FPSs for synthetic events (Table 6) are: reverse faulting for boundary between Alps and Friuli plain (faults 10, 11) and boundary between Alps and Dinarides (faults 12, 16), they have left-lateral strike-slip component in the western part (fault 11). Adriatic coast (faults 6-9), Idrija line (fault14) and eastern boundary of the structure (faults 3-4) shows reverse faulting with considerable right-lateral strike-slip component. Synthetic earthquakes in the Periadriatic line (fault2) show right-lateral strike-slip mechanism, and in the western boundary of the structure (fault 1) they are left-lateral strike-slip. This is in correspondence with the available observations that are given in Table 8.

Table 8. Correspondence between observed and synthetic FPS

<i>Fault</i>	<i>Synthetic FPS</i>	<i>Observed FPS</i>	<i>Fault</i>	<i>Synthetic FPS</i>	<i>Observed FPS</i>
1	-5	-4	9	135	142
2	-170	-179	10	105	95
3	115	112	11	65	78
4	125	97	12	95	
5	-	-	13	-	
6	125	-	14	130	148
7	107	-	15	140	
8	140	-	16	100	72

The analysis of the result of modeling demonstrates its good correspondence to observations. Velocities in the block structure are similar to GPS data (D'Agostio et al., 2005, Nocquet & Calais, 2003). The frequency-of-occurrence plot for synthetic seismicity has the same slope, as for observed one. The distribution of synthetic epicenters recovers main features of

recorded seismicity. The relative level of seismic activity in the different parts of region, as well as FPS does not contradict to the observations.

7. Synthetic and historical strong seismicity of Alps-Dinarides junction zone: Discussion.

7.1. Maximum modeled magnitude

The maximum magnitude of the synthetic earthquake is 7.4. This value is larger than maximum observed instrumental magnitude 6.5 given in UCI. Nevertheless, the number of investigators gives the data about historical events with the magnitude more than 7. Shebalin et al. (1998) reports 7.9 in 1348, 7.4 in 1511 and 7.5 in 1690 (table 1). Westaway (1992) estimate the magnitude of 1348 as $M=7.6$, and 1511 as 7.0 basing on the isoseismal maps of Postpischl (1985b). Probably, the value of $M=7.9$ is overestimated, nevertheless, very likely earthquakes of 1348 and 1511 had magnitudes more than 7. Magnitude 7.5 of 1690 is very disputable, as is estimated less than 6 in two of four used catalogs UCI, and CPTI, and has undetermined magnitude in NEIC. The equivalent magnitude of the instrumentally recorded Friuli series (1976) is estimated more than 7. This fact confirms that the structure is powerful to generate earthquake with magnitude 7 or more, in spite of the absence of reliable instrumentally recorded data. So the value of maximum possible magnitude 7.4 looks credible.

7.2. Recurrence period of large earthquakes

Let us consider the frequency-of occurrence plot of obtained synthetic seismicity (Figure 4). The earthquakes with magnitude less than 7 fit well to the linear part of plot. Starting from magnitude 7 the graph goes sharply down. It means that earthquakes with magnitude 7 or more are rare extreme events in the region under study, and we pay special attention to considering of such events in our discussion.

Model generates 140 earthquakes with magnitude more than 7 during the period 75 thousand of years; it is about 2 earthquakes per 1000 of years. The time sequence of magnitude 7 and more earthquakes is given in the Figure 7. They occur non-periodically. The plot in Figure 8 displays the number of such earthquakes in the sliding window 1000 yr with the step 200yr. This number varies from 0 to 6. The distribution of inter-event time is presented in Figure 9. It has small maximum in the time 0-200 years and then is quite homogeneous from 250 to 900years, and sometimes large intervals, almost 2000 years, occur. The results of modeling do not contradict the available observation. Shebalin et al (1998) gives 3 extreme events during 1000 years, i.e. 1348, 1511 and 1690. Intervals between these events are 163 and 179 years, that fits

well to the values obtained from modeling. Other investigators (Peresan & Panza .2002, Gruppo di lavoro CPTI, 2004) do not report 7 magnitude earthquakes; and this can not be rejected by the results of modeling, because there are long periods without extreme synthetic events.

The recurrence rate for earthquakes of lesser magnitude corresponds well to the observations. Model generates 2317 earthquakes with magnitude more than 6, i.e. 3 events per 100 yr, and 728 events with magnitude more than 6.5, i.e.1 event per 100yr. We suppose that magnitude 6 is presented completely in UCI in XX century. It reports 1 event with magnitude 6.5 and 7 events with magnitude more than 6; 4 of them are Friuli series of 1976, i.e. there are 4 independent earthquakes. As distinct from the result for extreme events, it is an expected trivial result, as we rescale the duration of synthetic catalog in correspondence with seismic activity rates using linear part of frequency-of-occurrence relation.

7.3. Possible locations of strong events.

The map of synthetic seismicity is given in Figure 5. The results of modeling proposed that large earthquakes with magnitude 6 and more can occur everywhere at the southern boundary of Alps (segments faults 10, 11, 12, 16); in the Alpine part of the region magnitudes 6 and more occur in the eastern segment of Periadriatic line (fault 2, segment 3) and at the eastern boundary of structure (fault 3). In the Dinaric part magnitude 6 and more earthquakes occur at the boundary of Dinarides and Adriatic marine basin (faults 6, 7, 8, 9), in the Idrija line (fault 14, segment 23), and in the northern segment of boundary between Dinarides and Pannonian basin (fault 4). I.e. earthquake with magnitude 6 can occur over almost all territory, excluding small parts of region in the north-west and south-east. Many of the locations determined by the modeling were already experienced by earthquakes with magnitude 6 and more (Figure 2 and Table 1).

The most interesting problem is possible location of extreme earthquakes with magnitude 7 and more. The model generates most of extreme events, 97 out of 140, at the southern boundary of Alps; they occur along the all boundary. Most active is the boundary between Alps and Dinarides. Maximum magnitude riches 7.25 between western boundary of Dinarides and Idrija line (fault 16, segment 26), and 7.4 to the east of Idrija (fault 12, segment 20). The numbers of events are 30 and 49 at the western and eastern segments respectively. Boundary between Alps and Friuli plain is less active; 18 synthetic earthquakes with magnitude more than 7 are obtained here; 6 of them sit at the most western segment (fault11, segment 15), maximum magnitude is 7.1. Only two extreme events were generated at the Friuli segment (fault 10, segment 14), in spite of its high seismic activity (i.e. number of synthetic events, see Table 6); maximum magnitude is 7.0. Possibly this segment is not able to generate many earthquakes with magnitude

7, as an extreme event is realized as several shock of lesser magnitude, that is reflected by block structure modeling. Figure 10 demonstrates the fragment of temporal sequence of synthetic earthquakes with magnitude 6 and more obtained for Friuli segment during 10000 years. Almost all of them occur in groups. Figure 10 (A, B) gives two examples of such series in details (duration is 1 year). The indirect confirmation of this hypothesis is Friuli series of 1976, when 4 earthquakes with magnitude more then 6 occurred during half of year.

The model generates 22 earthquakes with magnitude more than 7 at the western boundary of Dinarides. 17 events are located in the southern part, in the Adriatic coast to the east of Istria peninsula (fault 6, segment19); maximum of synthetic magnitude is 7.0 .Epicenters of 1323, 1721, and probably 1870 (table 1) are located in this zone. Four events with magnitude 7.0 and more occurred in the fault 8 (segment 11) very close to Trieste; obtained maximum magnitude is 7.15. Significant events are not known here. And one event with magnitude 7.05 sit in the fault 9 (segment 12), north from Udine; here is the epicenter of 1511.8.

Fourteen extreme events are generated at Idrija line; maximum magnitude is 7.4. Fitzko et al. (2005) found constraints in the northern part of Idrija line that are consistent with the epicenter of the 1511.3.

Six synthetic earthquakes with magnitude 7 and more occur at the boundary between Dinarides and Pannonian basin; maximum magnitude is 7.2. One is in the fault 3 (segment 5), near Ljubljana. Here is the epicenter of 1963. Five events sit in the fault 4 (segment 6); Epicenters of 576 and 1093 are here.

The observed historical earthquakes, candidates to be 7, are earthquakes of 1348, 1511.3 and 1690. The location of 1348, probably strongest event in the region, is very uncertain – the difference in the epicenter determination is about 100 km; that is large value in the scale of the region. Shebalin et al., (1998) and Postpischl (1985a) placed it in the eastern segment of Periadriatic line. Hammerl (1994) re-located the 1348 event from Carinthia to Friuli; Peresan&Panza give the epicenter in the boundary of Asps and Dinarides. The epicenter of 1511.3 is located near the intersection of Idrija line and boundary between Alps and Dinarides. . Fitzko et al. (2005) place it in the north of Idrija. Epicenter of 1690 is at the eastern part of Periadriatic line, but only Shebalin et al. (1998) prescribe magnitude more than 7 to this event, in other sources of data used in the present study its magnitude is estimated less than 6.

As it was shown above, the model generates a lot of extreme events at the boundary between Alps and Dinarides and in Idrija line, but not in the Periadriatic line. The obtained from the modeling maximum magnitude is 6.7 here (Table 5).

8. Comparison of the results of block structure modelling and recognition of seismogenic nodes

The spatial distribution of synthetic seismicity resulted from the block structure modelling is compared with the distribution of nodes prone to earthquakes with $M \geq 6.0$ (seismogenic nodes). The nodes have been identified in the region under consideration by means of pattern recognition applied to morphostructural zonation (Gorshkov et al., 2009). This methodology treats the nodes, which are formed around the intersections of the crustal block boundaries, as earthquake-controlling structures. The location and geometry of the nodes has been delineated in the Alps–Dinarides junction zone on the base of large-scale cartographic sources and the seismogenic nodes have been identified (Gorshkov et al., 2009). The area considered by Gorshkov et al. (2009) covers only blocks I to IV of the block model studied here.

The direct comparison of the block modelling results with the seismogenic node recognition is not straightforward since, in the block model (see part 4), the epicentre is determined as the centre of mass of the ruptured cells involved into an earthquake. Actually each of the largest synthetic earthquake breaks a whole segment or most of it, thus its epicentre coincide, by definition, with the geometric centre of the relevant segment, and certainly not with the intersections of the faults corresponding to MSZ nodes. Therefore the standard definition of synthetic epicentres used in the comparison with seismogenic nodes at 1:1.000.000 scale carried out studying region of Italy and its surroundings (Peresan et al., 2007), turns out not satisfactory at a more detailed scale used or the definition of the shape of each node (1:150.000). To allow the synthetic epicentres to be located at the intersection of lineaments, we propose the formal rule that assigns each earthquake to a certain node in a unique way. The rule is illustrated in Figure 11.

Each MSZ node is located within a vicinity of a rib, a line segment connecting corresponding vertices on the upper and the lower planes of the block structure. Let an epicentre belong to a fault segment bordered by ribs I and II (Fig. 11). We determine distances d_1 and d_2 between the epicentre and ribs I and II, respectively. An earthquake is assigned to the node I if $d_1 < d_2$ (earthquake 1 in Fig. 11) and to node II if $d_1 > d_2$ (as earthquake 2 in Fig. 11). Among the different synthetic earthquakes that fall into a given node we chose the one with the largest magnitude.

The comparison of results is shown in Figure 12 where epicentres of the synthetic earthquakes, with magnitude $M \geq 6.0$, and nodes delineated by Gorshkov et al. (2009) are shown. Four out of sixteen nodes delineated by Gorshkov (2009) and corresponding to the intersections of the third rank lineaments are not shown as we do not use lineaments of the third rank outlining the block structure geometry, and these excluded nodes do not correspond to the

vertices of the block structure; only one excluded node is seismogenic. The seismogenic nodes for $M \geq 6.0$ are bordered by solid line, the non-seismogenic ones – by dashed line. Of the twelve nodes shown, nine are seismogenic and three are non-seismogenic for $M \geq 6.0$.

The maximum magnitudes of the synthetic earthquakes assigned to nodes 1 to 12 are given in Table 9. The block modelling and the seismogenic node recognition differ only in nodes 5 and 10 that are recognized as non-seismogenic.

Table 9. Comparison of the results of block modeling and seismogenic nodes recognition (Gorshkov et al., 2009)

Node	Seismogenic nodes recognition	Maximum magnitude of synthetic earthquake	Comparison
1	NO	No earthquakes	+
2	YES	6.0	+
3	YES	6.6	+
4	YES	7.1	+
5	NO	7.1	-
6	YES	7.2	+
7	YES	7.4	+
8	YES	7.4	+
9	YES	6.9	+
10	NO	7.2	-
11	YES	7.4	+
12	YES	7.2	+

The partial disagreement between the results obtained by the modeling and recognition methods may be explained by both: inaccuracy of the recognition, and the rough description of the region in the model. The error rate in the recognition results is usually about 20%. After publication of the results of the recognition for the studied regions, eighty four large earthquakes occurred in these regions and fifteen of them (18%) occurred outside the nodes recognized as seismogenic (Gorshkov et al., 2003). This statistic reflects the errors of the first type “failure-to-predict”, while the errors of the second type “false alarm” cannot be checked by the available observations because of the short period of test in comparison with the inter-event time of large earthquakes. The results of the block structure modeling demonstrate that two out of twelve nodes (5 and 10) are “failures-to-predict”, i.e we have 17% of errors, and no “false alarm”. Therefore the discrepancy between block modeling and nodes recognition results can be considered equivalent to the discrepancy between recognition results and observed seismicity.

9. Conclusions

The junction zone of Alps and Dinarides is one of the most seismically active territories in Europe. It has a long history of the seismicity monitoring and is intensively investigated in last time. Nevertheless, the estimation of maximum possible magnitude, location and recurrence period of the strongest earthquakes is still open problem, as the duration of the instrumental observations is short, and historical data based on the macroseismic observations suffer from incompleteness and low accuracy of magnitudes and epicenters determination. The recurrence period of extreme events in the certain zone can be several thousands of years, that is much longer than period of observation even including historical data.

We use the block structure model to study long-term characteristics of strong seismicity. The synthetic earthquake catalog with equivalent duration 75 thousand of years was generated, and we analyze simultaneously the synthetic and historical strong seismicity. Model recovers the main features of observed seismicity and kinematics in the region: the rates and directions of tectonic movements are in correspondence with GPS observations. The distribution of epicenters, b -value, relative levels of seismic activity in the different parts of region as well as fault plane solutions are similar for recorded and synthetic earthquakes.

The results of modeling allow determine extreme events; they are earthquakes with magnitude $M \geq 7$ as they do not fit to the linear part of frequency-of-occurrence plot. The rate of such earthquakes is a bit less than 2 events per 1000 years. The maximum magnitude of synthetic earthquakes is 7.4, and it does not contradict to available historical observation.

The most part of extreme synthetic events sit at the southern boundary of Alps, where highest level of recorded seismic activity is observed. Another large group of extreme events are at the Adriatic coast, to the east of Istria peninsula. Several synthetic earthquakes with magnitude more than 7 were generated in Idrija line, and at the eastern and western boundaries of Dinarides. Many of these locations have been already experienced by significant earthquakes with magnitudes more than 6. Modeling proposes a number of possible locations of extreme events where large earthquakes were not observed before; in particularly at the western boundary of Dinarides sit four extreme events near Trieste.

The space distribution of strong synthetic earthquake epicentres is compared with recognition of seismogenic nodes (Gorshkov et al., 2009) The results obtained by two methods are similar for the most part of studied territory. The partial disagreement between the results obtained by two methods may be explained by both: inaccuracy of the recognition, and the rough description of the region in the model. The discrepancy is similar with that one between the recognition results and the observed seismicity.

The block structure modeling does not pretend to reflect the reality in all details. It supposes simplified description of the region: the blocks are perfectly rigid, and faults are infinitely thin planes. Model does not describe in details the regional fault network, and the single fault in the model represents the whole fault zone. The external tectonic movements supposed to be stationary that can not be checked due to very short period of GPS observations. Nevertheless, the model reproduces correctly many features of regional seismicity and kinematics that is checked against the available observation. It allows suppose that presented result reflects correctly the maximum magnitude, recurrence time, and possible locations of largest earthquakes in the junction zone of Alps and Dinarides, and it can be useful for estimation of the seismic hazard and seismic risk assessment.

References

- A. Aoudia, A. Sarao, B. Bukchin, and P. Suhadolc (2000) *The 1976 Friuli (NE Italy) Thrust Faulting Earthquake: A Reappraisal 23 Years Later*. Geophysical Research Letters, VOL. 27, NO. 4, PAGES 573-576, 2000
- J. Bajc, A. Aoudia, A. Sarao, and P. Suhadolc (2001). *The 1998 Bovec-Krn mountain (Slovenia) earthquake sequence*. Geophysical Research Letters, VOL. 28, NO. 9, PAGES 1839-1842, 2001
- Camassi, R., and Stricchi, M. (1996) *NT 4.1 un Catalogo Parametrico di terremoti di Area Italiana al di sopra della soglia di danno*, CNR-GNDT. <http://emidius.mi.cnr.it/NT/home.html/>
- Carulli G.B., Nicolich R., Rebez A. & Slejko D. (1990) - Seismotectonics of the Northwest External Dinarides. *Tectonophysics*, **179**, 11-25.
- Chimera, G., Aoudia, A., Saraò, A., and Panza, G. F. (2003), *Active tectonics in Central Italy: constraints from surface wave tomography and source moment tensor inversion*, Phys. Earth Planet. Inter. *138*, 241-262.
- S. Cloetingh, T. Tornu, P.A. Ziedler, F. Beekman. (2006) *Neotectonics and intraplate topography of the northern Alpine Foreland*. Earth-science Reviews *74*) p127-196, 2006
- M. Cuffaro, E. Carminati, and C. Doglioni (2006). *Horizontal versus vertical plate motions*. eEarth Discuss., 1, 63–80, 2006. www.electronic-earth-discuss.net/1/63/2006/
- N. D'Agostino, D. Cheloni, S. Mantenuto, G. Selvaggi, A. Michelini, and D. Zuliani. (2005) *Strain accumulation in the southern Alps (NE Italy) and deformation at the northeastern boundary of Adria observed by CGPS measurements*. Geophysical Research Letters, VOL. 32, L19306, doi:10.1029/2005GL024266, 2005

- DOGLIONI C. (2000) - *Sismotettonica dell'Italia nord-orientale e possibile comparazione con gli Appennini*. In: GALADINI F., MELETTI C. & REBEZ A. (Eds), *Le ricerche del GNDT nel campo della pericolosità sismica (1996-1999)*, CNR-Gruppo Nazionale Difesa Terremoti, Roma, 51-58.
- FPS DST data file (2006)
- FITZKO, F., SUHADOLC, P., AOUDIA, A., PANZA, G.F., 2005. Constraints on the location and mechanism of the 1511 Western-Slovenia earthquake from active tectonics and modeling of macroseismic data. *Tectonophysics*, **404**, 77–90.
- GABRIELOV, A. M., LEVSHINA, T. A., AND ROTWAIN, I. M. 1990. *Block model of earthquake sequence*, *Phys. Earth Planet. Inter.* **61**, 18-28.
- GORSHKOV A., KOSSOBOKOV V. AND SOLOVIEV A., 2003. Recognition of earthquake-prone areas. In: *Nonlinear Dynamics of the Lithosphere and Earthquake Prediction* (V.KEILIS-BOROK AND A. SOLOVIEV, eds.). Springer, Heidelberg, 239-310
- GORSHKOV A.I., PANZA G.F., SOLOVIEV A.A., AOUDIA A. (2004). *Identification of seismogenic nodes in the Alps and Dinarides* Bolletino della Societa Geologica Italiana, **123**, 3-18.
- GORSHKOV A.I., PANZA G.F., SOLOVIEV A.A., AOUDIA A., PERESAN A. 2009 *Delineation of the geometry of the nodes in the Alps-Dinarides hinge zone and recognition of seismogenic nodes ($M \geq 6$)*. *Terra Nova*, Vol. 21, No. 4, 257–264
- GRUPPO DI LAVORO CPTI (2004). *Catalogo Parametrico dei Terremoti Italiani, versione 2004 (CPTI04)*, INGV, Bologna, <http://emidius.mi.ingv.it/CPTI04/>
- HAMMERL, C., 1994. The earthquake of January 25th, 1348: discussion of sources. In: *Historical investigation of European earthquakes* (P. Albini and A. Moroni, eds) C.N.R. 1st.Ric. Rischio Sism., Milano.
- JIMENEZ-MUNT, I., SABADINI, R., AND GARDI, A. (2003), *Active deformation in the Mediterranean from Gibraltar to Anatolia inferred from numerical modeling and geodetic and seismological data*, *J. Geophys. Res.* **108** (B1), 1-24.
- MELETTI C., PATACCA E. & SCANDONE P. (2000) - *Construction of a seismotectonic model: the case of Italy*. *Pure Appl. Geophys.*, **157**, 11-35.
- NEIC Hypocenter data file. <http://neic.usgs.gov>
- NOCQUET, J. M., AND CALAIS, E. (2003), *Crustal velocity field of western Europe from permanent GPS array solutions, 1996–2001*, *Geophys. J. Int.* **154**, 72–88.
- PANZA, G. F., RAIKOVA R. B.(2008) *Structure and rheology of lithosphere in Italy and surrounding*. *Terra Nova*, **20**, 194–199
- PERESAN, A. AND PANZA, G. F. (2002), *UCI2001: The Updated Catalogue of Italy*, ICTP, Trieste, Internal report, IC/IR/2002/3, and its updates.

- PERESAN, A., I. VOROBIEVA, A. SOLOVIEV, G.F. PANZA. *Simulation of Seismicity in the Block-structure Model of Italy and its Surroundings*. Pure Appl. Geophys., **164**, 2193-2234.
- POSTPISCHL, D.(1985A) *Catalogo dei terremoti Italiani Dall'Anno 1000 al 1980*. Consiglio Nazionale delle Ricerche, Rome, Italy, 1985. pp239
- POSTPISCHL, D.(1985B) *Atlas of isoseismal maps of Italian Earthquakes*. Consiglio Nazionale delle Ricerche, Rome, Italy, 1985. pp164.
- PRELOGOVIĆ E., SAFTIĆ B., KUK V., VELIĆ J., DRAGAŠ M. & LUČIĆ D. (1998) - *Tectonic activity in the Croatian part of the Pannonian basin*. Tectonophysics, **298**, 283-293.
- SHEBALIN, N., LEYDECKER, G., MOKRUSHINA, N., TATEVOSIAN, R., ERTELEVA, M., & VASSILIEV, V. (1998) - *Earthquake catalogue for Central and Southeastern Europe 342 BC - 1990 AD*. European Commission, Report No. ETNU CT 93-0087, Brussels.
- SOLOVIEV, A., AND ISMAIL-ZADEH, A. (2003), *Models of dynamics of block-and-fault systems*, In *Nonlinear Dynamics of the Lithosphere and Earthquake Prediction* (eds. Keilis-Borok, V. I., and Soloviev, A. A.) (Springer-Verlag, Berlin-Heidelberg) pp. 71-139.
- ŠUŠTERŠIČ, F., 1996 *Poljes and caves of Notranjska*. Acta Carsologica, 25, 251-289
- WESTAWAY, R. (1992) *Seismic moment Summation for Historical Earthquakes in Italy: Tectonic Implications*. Journal of Geophysical research. Vol. 97, No B11, 15,437-15,464.
- ŽIVČIČ, M., SUHADOLC, P., VACCARI, F., 2000. Seismic zoning of Slovenia based on deterministic hazard computations. *Pure Appl. Geophys.* **157**, 171– 184.

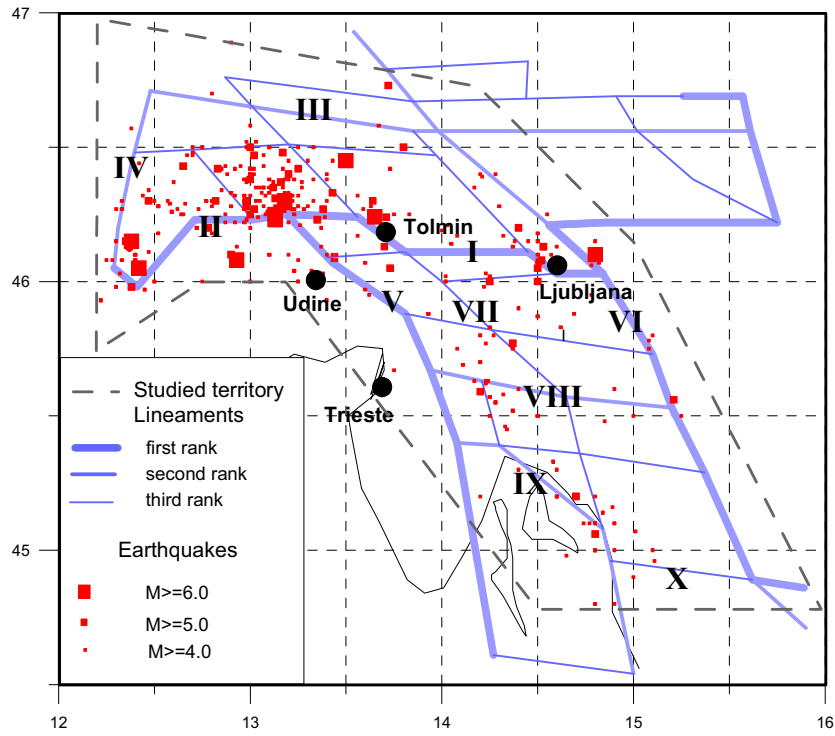


| Figure 1. Seismicity of the Friuli region (Peresan and Panza. 2002), from 1000 to 2006, -and the morphostructural zoning (Gorshkov et al., 2004)

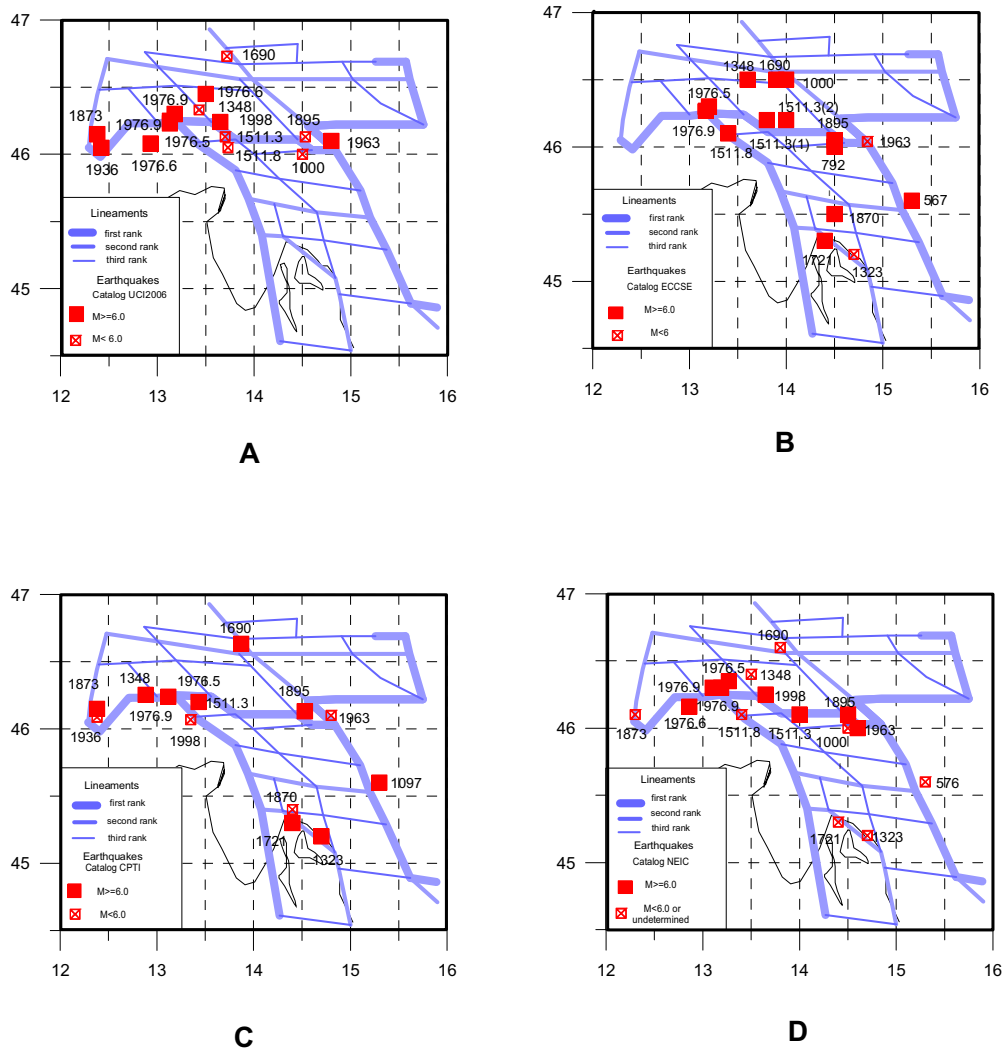


Figure 2. Significant earthquakes in junction zone of Alps and Dinarides by four sources of data. A. Catalog UCI, 1000 - 2006 (Peresan & Panza, 2002); B “Earthquake catalogue for Central and Southeastern Europe 342 BC - 1990 AD”, (SHEBALIN et al., 1998); C. “Catalogo Parametrico dei Terremoti Italiani (CPTI04)”1000 - 2004, (Gruppo di lavoro CPTI, 2004); D. NEIC, Significant Earthquakes World Wide Data file. 500 - 2006

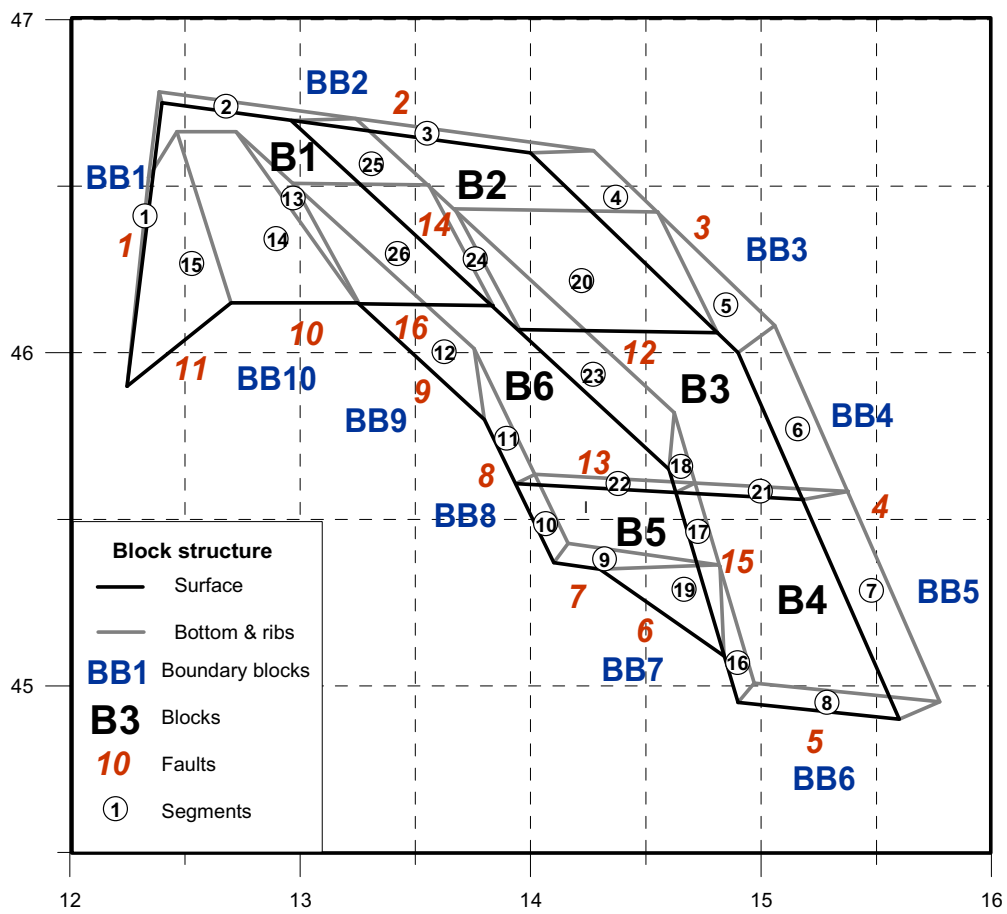


Figure 3. Geometry of the block structure outlined on the base of the morphostructural map (Gorshkov et al., 2004)

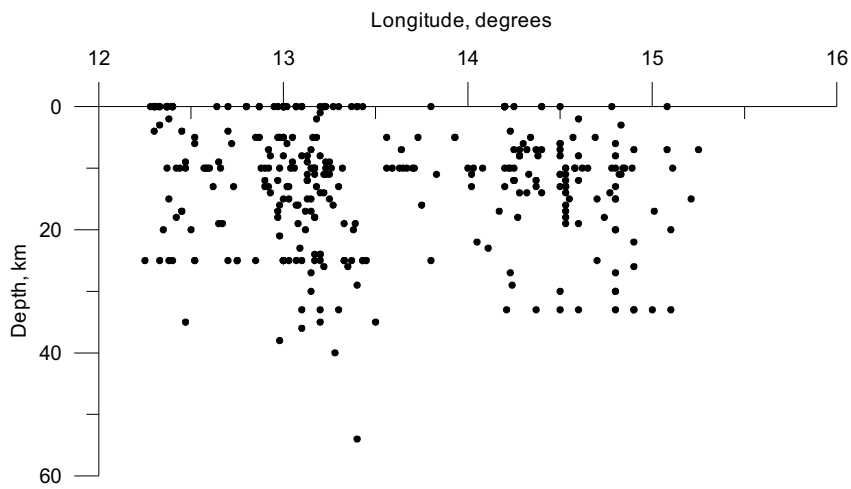


Figure 4. Distribution of seismicity in the depth UCI (Peresan and Panza 2002)

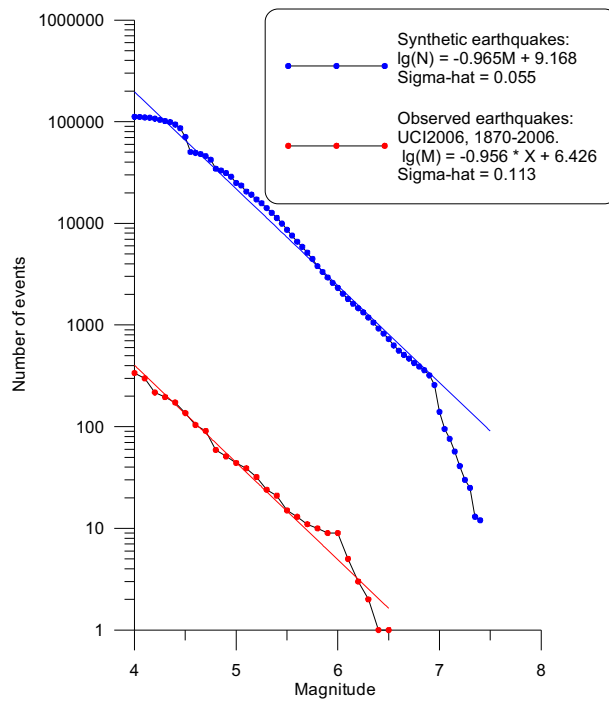


Figure 4. Gutenberg-Richter plots for observed and synthetic seismicity

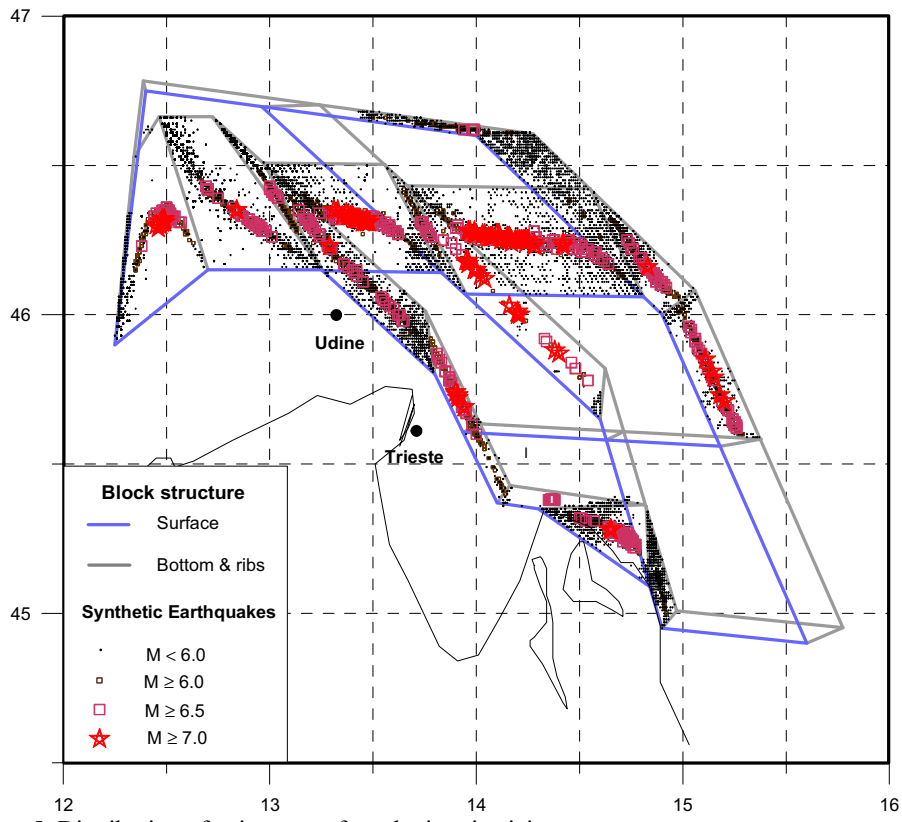


Figure 5. Distribution of epicenters of synthetic seismicity.

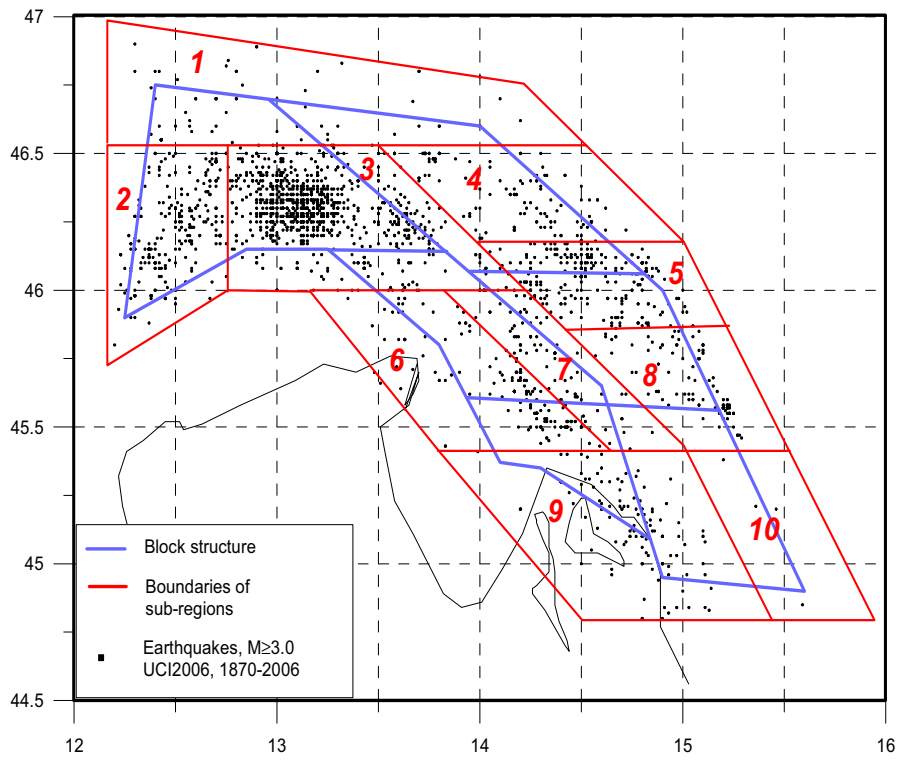


Figure 6. Ten sub-regions and observed seismicity with $M \geq 3$, catalog UCI, 1870-2006

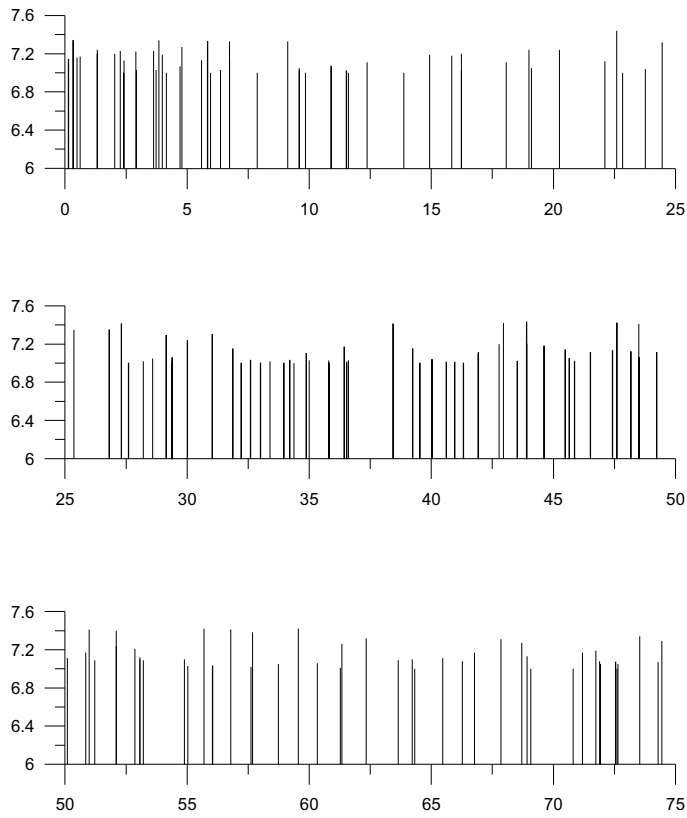


Figure 7. Temporal sequence of synthetic earthquakes with magnitude $M \geq 7$.

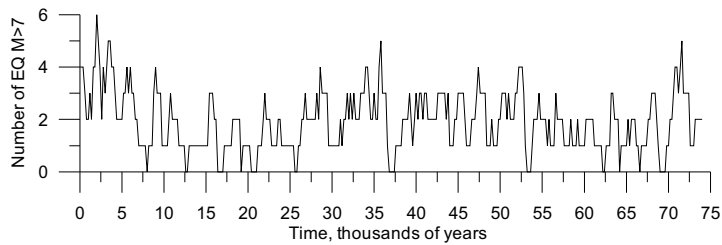


Figure 8. Number of synthetic earthquakes with magnitude $M \geq 7$ in the sliding window 1000 years.

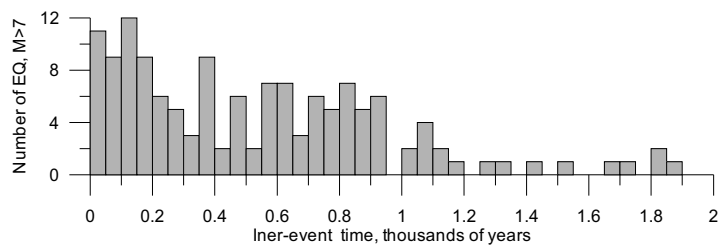


Figure 9. Distribution of inter-event times of synthetic earthquakes with magnitude $M \geq 7$.

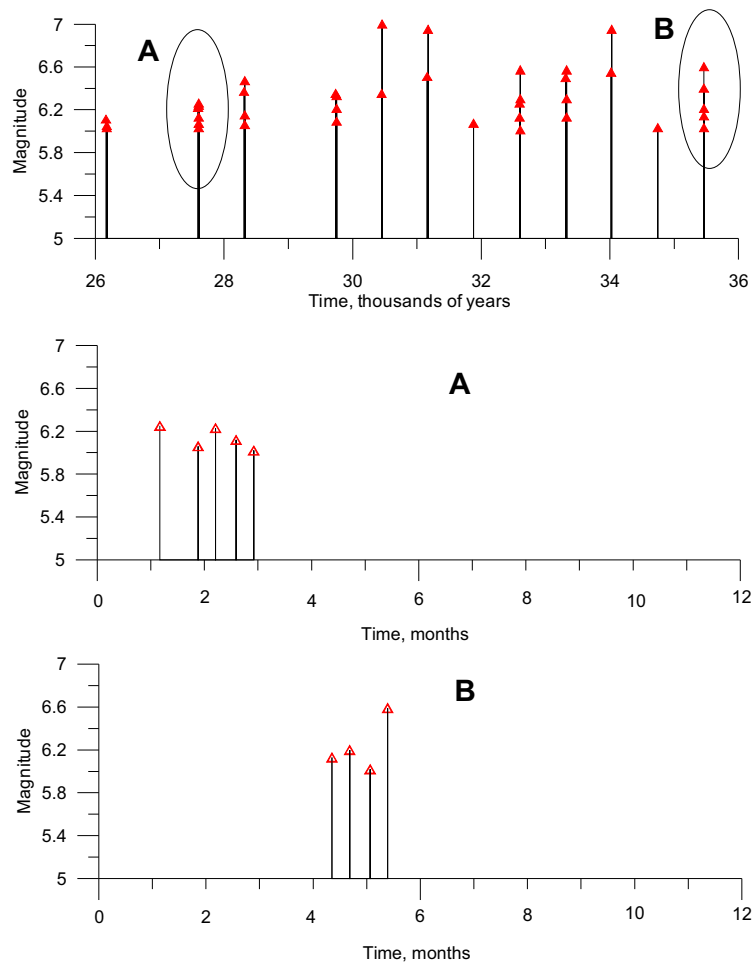


Figure 10. Temporal sequence of earthquakes with magnitude 6 and more in Friuli segment. During 10000 years; A,B. – fragments, duration 1 year.

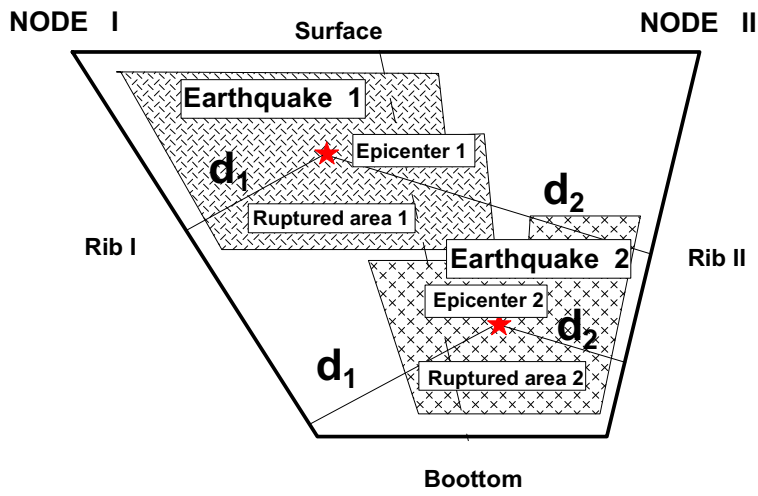


Figure 11. Assignment of a synthetic earthquake to a node.

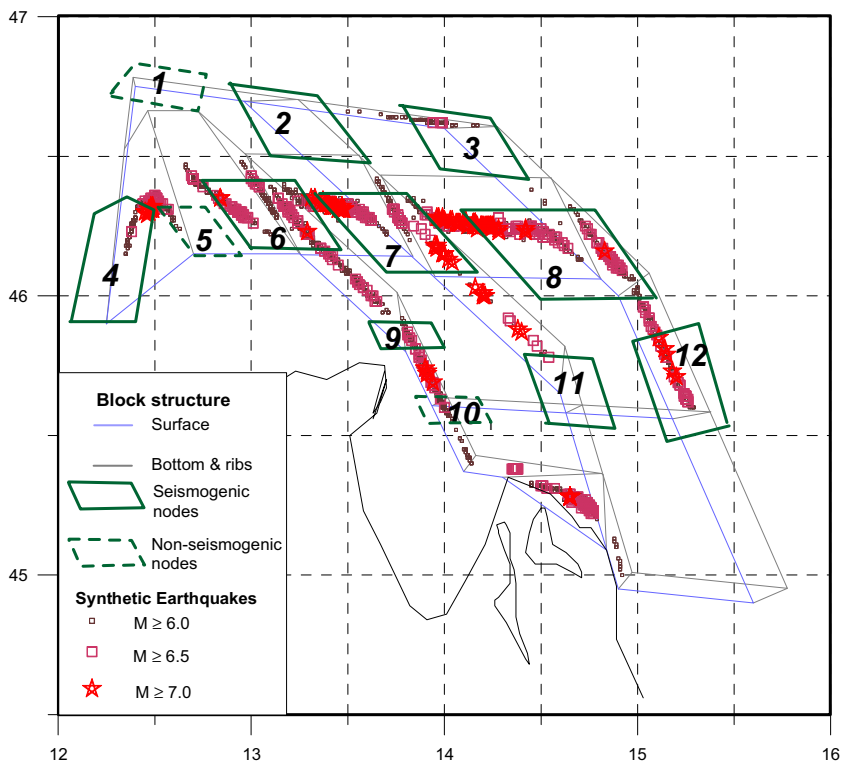


Figure 12. Synthetic seismicity with magnitude $M \geq 6.0$ and nodes of the morphostructural scheme (Gorshkov et al., 2009)